

## **A Study on the Coolant Mixing Phenomena in the Reactor Lower Plenum**

**Yong Seog Choi and Goon Cherl Park**

Seoul National University  
San 56-1, Shinlim-dong, Kwanak-gu, Seoul 151-742, Korea

**Kil Sup Um**

Korea Atomic Energy Research Institute  
150 Dukjin-dong, Yusong-gu, Taejon 305-353, Korea

(Received May 12, 1996)

### **Abstract**

When asymmetric thermal-hydraulic conditions occur between cold legs, the core inlet temperature will be nonuniform if the coolant is not mixed perfectly in the lower plenum. These uneven core inlet conditions may induce the change in core power distribution. Thus realistic prediction of thermal mixing is important in such abnormal conditions. In this study, reactor internals, which are scaled down as to conserve the flow area ratio, are set up in the model of KORI Unit 1 with the scaling factor of 1/710 by volume and coolant temperatures are measured beneath the lower core plate. Based on experimental results, the ability of COMMIX-1B code to simulate the coolant mixing phenomena in the lower plenum is estimated.

The results show that complete mixing never occurs in any conditions and the mixing pattern is characterized according to the plant type.

### **1. Introduction**

Asymmetric thermal-hydraulic conditions can develop between reactor cold leg loops due to instrumentation and control system uncertainties, steady perturbations in the steam generator secondary flow, or uncertainties of recirculation pump flow rates. Such steady-state asymmetric conditions can be sustained over a fuel cycle, and may alter the core power distribution and fuel burnup. More severe conditions can occur under transient situations such as a stuck-open relief valve on a steam generator, loss of or excessive feedwater to the steam generator, incapacity of a pump, or a steam line break. In the steam

line break accident, one or two steam generators are assumed to fail and steam generator isolation valves are assumed to be closed. This causes a rapid reduction in cold leg temperature for the loops with failed steam generator, and less rapid reduction of the remaining loop temperature. Such situations are concerned in safety problems. When such asymmetric thermal-hydraulic conditions exist between cold legs, the temperature and flow distribution will be nonuniform at the core inlet if the thermal mixing in lower plenum becomes imperfect. These uneven core inlet conditions may induce the change in core power distribution. Realistic prediction of core inlet conditions based on the proper understanding of the

thermal mixing in the lower plenum is thus important in providing realistic predictions of power tilts and recriticality potential in asymmetric cooling transients and hypothetical accidents.

There were two similar experiments. The one is thermal mixing test in the lower plenum of Oconee unit 1 conducted by EPRI and the other is mixing measurement in the IPP 1/7 model. Oconee unit 1 is a typical B&W PWR. There are two pumps and two cold legs on each of the two coolant loops so the coolant mixing behavior in the downcomer and the reactor internals in the lower plenum are different from domestic nuclear power plants[1,2]. Consequently it is difficult to adapt the results directly to domestic ones. The details of the IPP 1/7 test is impossible to obtain.

In this study, reactor internals to simulate the downcomer and the lower plenum are set up in the SNUTF-loop[3] which models the KORI Unit 1 with the scaling factor of 1/710 by volume. Loop flow conditions are measured at each loop and controlled by pump and steam generator secondary side con-

dition. The core inlet temperatures are measured beneath the lower core plate. With those test results, inlet coolant temperature maps are produced in various conditions and the aspect of flow mixing is estimated. Additionally the three-dimensional steady-state computations for the analysis of the thermal mixing tests are performed using COMMIX-1B code.

## 2. Description of Test Facilities

### 2.1. Pressure Vessel

KORI Unit 1 is a Westinghouse pressurized water reactor, having two loops. Seoul National University has a test loop, named as SNUTF and shown in Fig. 1, which models the unit with the scaling factor of 1/710 by volume. The design parameters of SNUTF and KORI Unit 1 are listed in Table 1. Since the mixing phenomena in the lower plenum is a main concern in this study, the geometric similarity is maintained only in the lower plenum. The reactor internals

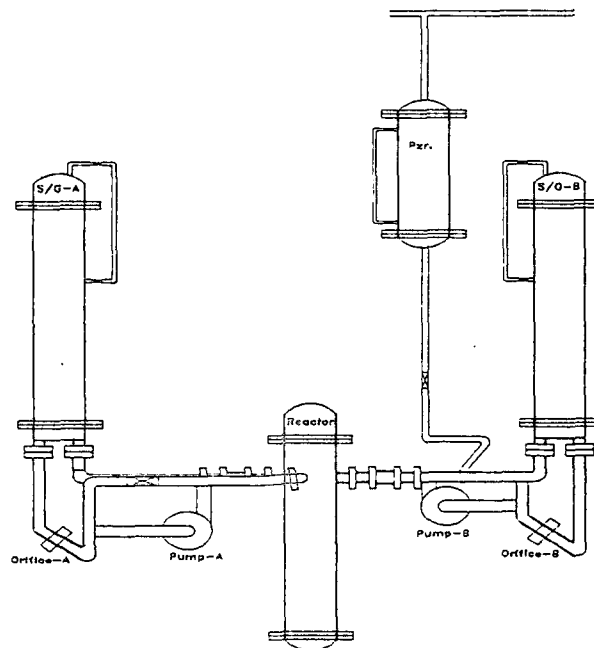


Fig. 1. Overall View of Test Facility

are scaled down as to conserve the flow area ratio and added in the original loop. The lower plenum internals are shown in Fig. 2. There are two types of instrumentation guide tube (Butt type & Cruciform) and a tie plate under the lower core support plate. There exist lower core support columns, diffuser plate and lower core plate over it. In the core region, in order to simulate pressure drop, thirty seven fuel assemblies are placed. Among them, twelve ones are electric heaters and other twelve ones take place of thermocouple guide tubes and upper core support columns. The U-shaped electric heaters are installed from upper head and has the heating length proportional to fuel assembly. Thermocouples are also installed from the upper head and coolant temperatures are measured beneath the lower core plate. In the upper plenum, there are upper core plate, upper core support plate and upper core support columns.

## 2.2. Steam Generator

Steam generators are the inverted U-tube shell-and-tube type. There are 16 U-tubes in each steam generator and made of copper pipe with 19 mm inner diameter. Primary and secondary systems are separated by 40 mm thickness tube sheet, hot and cold side of primary system by 30 mm thickness bulkhead[3].

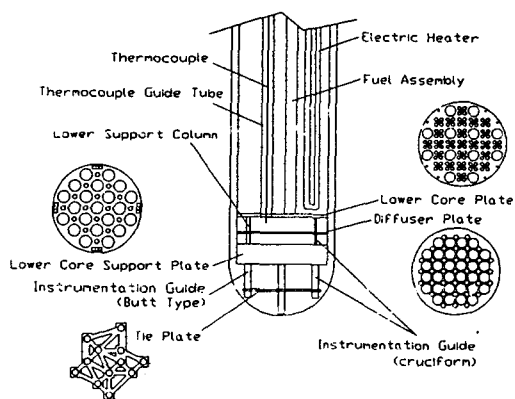


Fig. 2. Pressure Vessel and Reactor Internals

## 2.3. Pressurizer

Primary system pressure is maintained by boiling the water in the pressurizer. In the upper head safety

Table 1. Design Parameters of SNUTF and KORI Unit 1

Parameter	SNUTF	KORI Unit 1
No. of Loops (EA)	2	2
Max. Core Power (kW)	60	1728500
Max. Pressurizer Power (kW)	5	1000
Design Pressure (MPa)	1	16.9
Total Primary Volume (liter)	265.36	175213
Vessel		
Material	SUS 304	Carbon Steel
Height(mm)	1926	11896
I.D.(mm)	310	3352.8
Downcomer		
Material	SUS 304	Carbon Steel
Height (mm)	1320	-
I.D. (mm)	260	2768.6
Hot Leg		
Material	SUS 304	Stainless Steel
I.D. (mm)	70	736.6
Length (mm)	1270	
Suction Leg		
Material	SUS 304	Stainless Steel
I.D. (mm)	70	698.5
Length (mm)	2030	
Cold Leg		
Material	SUS 304	Stainless Steel
I.D. (mm)	70	698.5
Length (mm)	1160	
Steam Generator		
No. of S/G (EA)	2	2
No. of U-Tube (EA)	32	3388
Material	Copper	Inconel
I.D. of Tube (mm)	19	19.69
Avg. Length of Tube (m)	3266.25	23037.23
Heat Transfer Area (m <sup>2</sup> )	7.22	4784.51
I.D. of Shell (mm)	260	3285.74
Pressurizer		
Material	SUS 304	Carbon Steel
Height (mm)	920	-
I. D. (mm)	310	2133.6

valve which operates passively at 10 atm. and solenoid valve are attached to prevent the pressure rise over 10 atm. [3].

### 2.4. Coolant Pump

To keep hydraulic similarity in the lower plenum, volumetric flow rate of 40,000 liter/min is required. But such a flow rate is impossible for this test facility because of piping size. Present pump has the maximum flow rate of 380 liter/min.

### 2.5. Flow Rate Measurement

The flow rate of primary coolant is measured at the suction leg using a flange tapped orifice. The correlation for volumetric flow rate is as follow[4],

$$Q = C_d A_t \left[ \frac{2 \Delta p}{\rho (1 - \beta^4)} \right]^{1/2}$$

where,

$$C_d = f(\beta) + 91.71 \beta^{2.5} Re_D^{-0.75} + \frac{0.09 \beta^4}{1 - \beta^4} F_1 - 0.0337 \beta^3 F_2$$

$$f(\beta) = 0.5959 + 0.0312 \beta^{2.1} - 0.184 \beta^8$$

$$F_1 = F_2 = \frac{1}{D(in)} \quad D \geq 2.3 in$$

$\beta$ , the major design parameter of the orifice, is 0.55963 in this test facility.

### 2.6. Temperature Measurement

The coolant temperature is measured at the core inlet using T-type thermocouples installed from the upper head. It is composed of copper-constantan and available for temperature range of  $-200^\circ\text{C} \sim 400^\circ\text{C}$ .

The voltage signals from thermocouples are recorded through A/D converter after being amplified by AD595. It is a complete instrumentation amplifier and thermocouple cold junction compensator on a

monolithic chip. It combines an ice point reference with a precalibrated amplifier to produce a high level( $10\text{mV}/^\circ\text{C}$ ) output directly from a thermocouple signal and includes a thermocouple failure alarm that indicates if one or both thermocouple leads become open[5]. The A/D converter is IBM PC/AT compatible with resolution of 12 bit and maximum sampling rate of 100 kHz.

## 3. Experiments and Results

The objective of this test is to create a cold leg temperature mismatch between loops and monitor various temperatures at the core inlet.

To generate the cold leg temperature difference, one of two steam generators is isolated and the feed water of  $15^\circ\text{C}$  is supplied to the other one. Until the heat added from the core and removed in the steam generators are balanced, the cold leg temperature difference varies continuously. Therefore the mixing phenomena under various cold leg temperature differences is to be observed during such slow, nearly quasi-steady transition.

Fig. 3 shows the typical mixing pattern observed. A distinct border is formed in the center region. The isothermal line of 0.0 represents the average temperature of core inlet and the deviation from that is displayed in kelvin.

Test parameters are system pressure, flow rate, cold leg temperature difference( $\Delta T_c$ ) and the case of the flow rate mismatch between two loops is considered. To investigate the effect of diffuser plate, test without it is also conducted. To estimate the degree of mixing quantitatively we define the barometer like this.

$$\frac{\sigma}{\Delta T_c} = \frac{\text{standard deviation of core inlet temperature}}{\text{temperature difference between cold legs}}$$

This barometer has the maximum value of 0.5 theoretically. In most cases it has the almost uniform value of 0.24~0.28.

Test results shows that primary system pressure has no influence upon the mixing pattern as shown

in Fig. 3 and Fig. 4. Coolant flow rate rarely affects the mixing, but when considered together with the cold leg temperature difference, it has quite a little effects. When cold leg temperature difference is large and flow rate is low the mixing pattern is very different from the usual case. As shown in Fig. 5, the colder water rushes to the center region of the core inlet and the hotter water is pushed out. The reason for this is that when flow rate is high the coolant density difference has little effect on mixing pattern but in case of low flow rate driving force is not sufficient enough to overcome the buoyancy effect of coolant induced by temperature difference. In case of the flow rate mismatch between two loops (Fig. 6), the average temperature line is merely pushed to one side but coolant does not mix well, either. Diffuser plate also has little effect on the coolant mixing as shown in Fig. 7.

As mentioned in section 2.4 the hydraulic similarity could not be conserved because of the coolant pump capacity. In most experiments it is very difficult to conserve Reynolds number so the low-Reynolds-number model data are used to estimate by

extrapolation the desired high-Reynolds-number prototype data. Obviously there is considerable uncertainty in using such an extrapolation, but there is no other practical alternative in hydraulic model test-

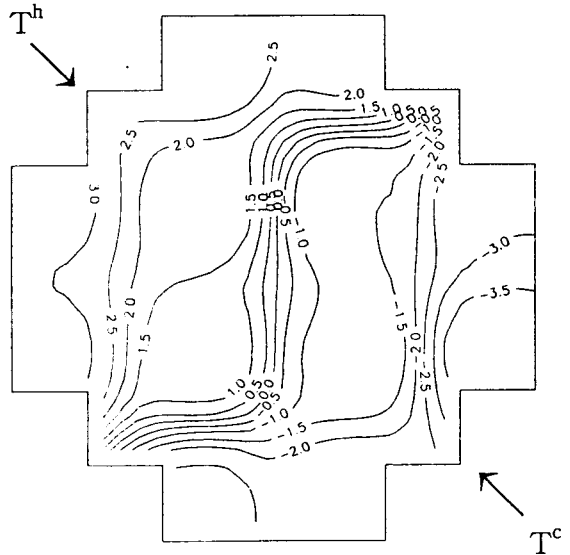


Fig. 4. Core Inlet Temperature Distribution  
(7atm., 310l/min,  $T^h = +5.8\text{K}$ ,  $T^c = -4.5\text{K}$ ,  
 $T_{avg} = 339.8\text{K}$ )

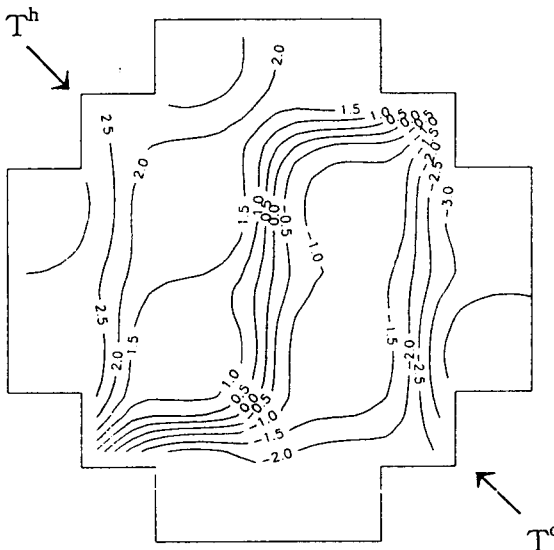


Fig. 3. Core Inlet Temperature Distribution  
(3atm., 310l/min,  $T^h = +5.7\text{K}$ ,  $T^c = -4.4\text{K}$ ,  
 $T_{avg} = 336.6\text{K}$ )

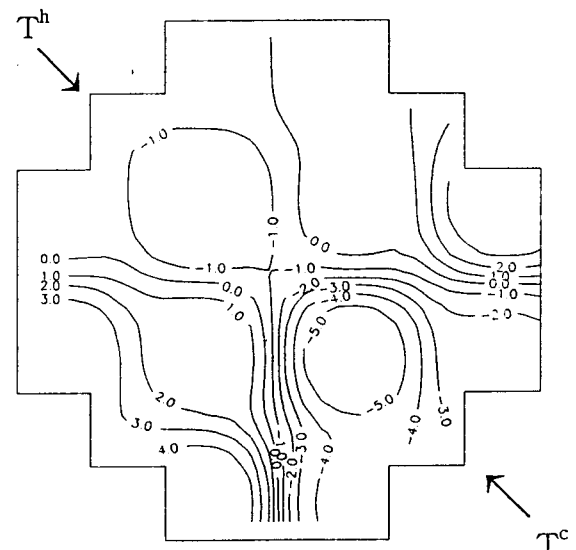


Fig. 5. Core Inlet Temperature Distribution  
(3atm., 180l/min,  $T^h = +12.5\text{K}$ ,  $T^c = -9.8\text{K}$ ,  
 $T_{avg} = 371.2\text{K}$ )

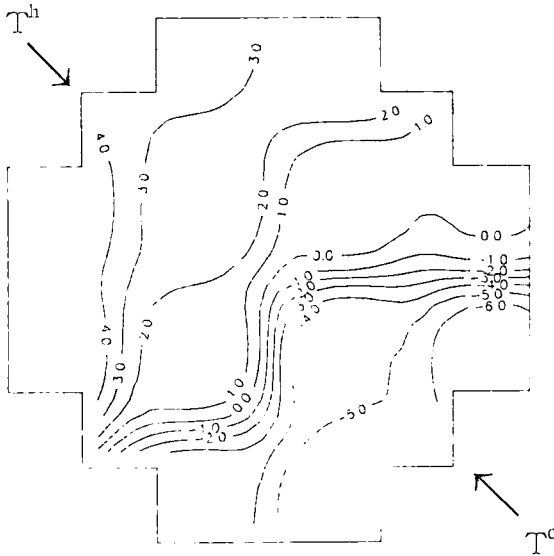


Fig. 6. Core Inlet Temperature Distribution  
(3atm., 310l/min, 180l/min,  $T^h=+7.3K$ ,  
 $T^c=-8.3K$ ,  $T_{avg}=362.9K$ )

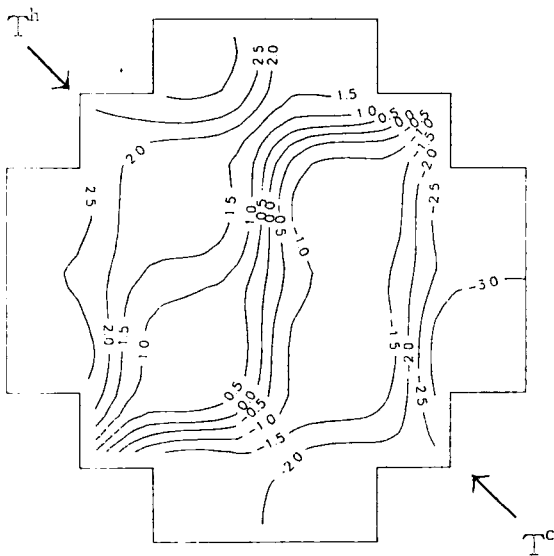


Fig. 7. Core Inlet Temperature Distribution Without Diffuser Plate  
(3atm., 310l/min,  $T^h=+5.6K$ ,  $T^c=-4.1K$ ,  
 $T_{avg}=336.8K$ )

ing[4]. The test results show that the mixing pattern is much the same upon the flow rate variation except

Table 2. Summary of Test Results

Test No.	Pressure (atm)	flow rate (l/min)	$\Delta T_c$ (°C)	$\sigma/\Delta T_c$
1	3	180	22.8	0.146
2	3	180	9.9	0.269
3	3	180	5.7	0.282
4	3	250	14.9	0.243
5	3	250	10.3	0.201
6	3	250	4.8	0.256
7	3	310	14.9	0.240
8	3	310	10.1	0.236
9	3	310	3.9	0.244
10	3	350	11.6	0.259
11	3	350	10.1	0.270
12	3	350	3.2	0.266
13	5	310	14.9	0.247
14	5	310	10.5	0.238
15	5	310	4.4	0.245
16	7	310	15.7	0.235
17	7	310	10.3	0.248
18	7	310	3.9	0.251
19	3	310, 180	15.6	0.258
20	3	310, 180	13.1	0.227
21	3	310, 180	5.2	0.262

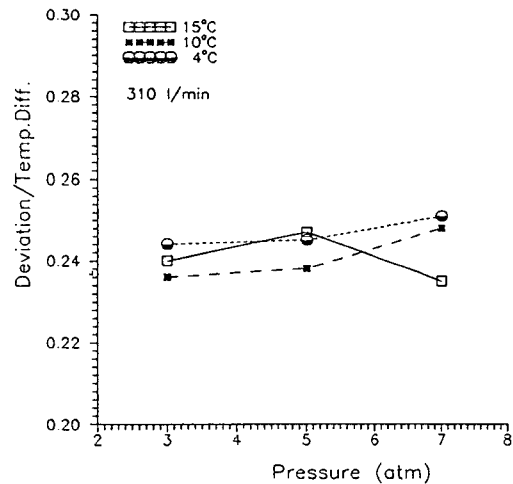


Fig. 8. The Effect of Pressure on the Mixing

the very low flow rate. Therefore it is predicted that the coolant does not mix well in the prototype, too.

Overall test results is shown in Table 2. The effect

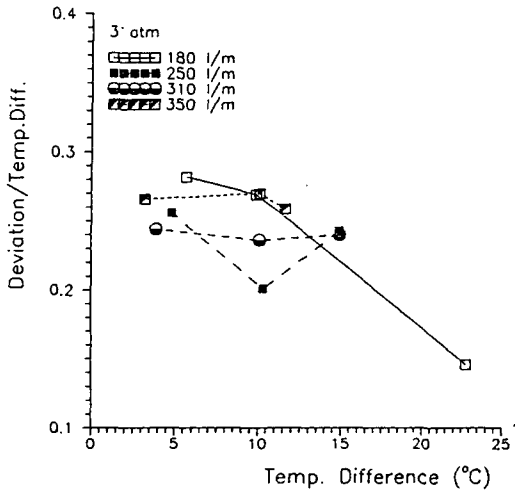


Fig. 9. The Effect of Temperature Difference on the Mixing

of test parameters on the barometer defined above is shown in Fig. 8 and Fig. 9. None of these parameter has the significant influence upon the coolant mixing.

#### 4. COMMIX-1B Calculation

To confirm the applicability of COMMIX-1B code to simulate the coolant mixing in the lower plenum, the computations for the analysis of the mixing tests were performed and the calculation results were compared with those of the mixing tests.

##### 4.1. Nodalization of COMMIX-1B

The node number of COMMIX-1B to simulate the mixing test is, as shown in Table 3 and Fig. 10, 8 for radial direction, 24 for axial direction and 24 for azimuthal angle and cylindrical coordinate is used. The axial node number of 5 is assigned to tie plate, 10~11 to lower core support plate, 13 to diffuser plate and 16 to lower core plate. Since the major concern is the temperature distribution at the core inlet, the modeling of core region, upper plenum and hot leg is excluded for the efficiency of the calculation.

The simulations were performed for the represen-

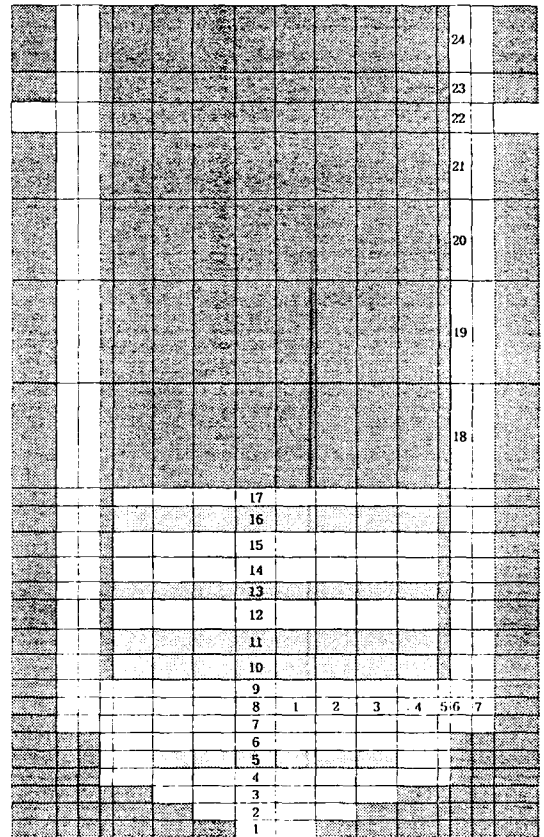


Fig. 10. Nodalization of COMMIX-1B for the Test Facility

tative cases of the test sets. The boundary conditions for each case is shown in Table 4.

##### 4.2. Calculation Results

The calculation results are shown in Fig. 11 and Fig. 12. The values at the 12 different points are test data and those in the parenthesis are temperature difference between test data and calculation results.

The reason why the results are somewhat different from each other is that in calculation complete insulation is assumed throughout the downcomer but there exists heat flow through baffle and barrel in the test facility. The isothermal lines in the test results are produced based on the experimental data of 12 points but those of the calculation results are yielded bas-

Table 3. Nodalization of COMMIX-1B for the Test Facility

Node Number	Radial Node (mm)		Azimuthal Node (radian)		Axial Node (mm)	
1	33		0.257436		12	
2	33	inside	0.244346		20	
3	33	annulus	0.270526	cold inlet nozzle	20	
4	32	inner wall	0.270526		20	
5	3	inner wall	0.244346		5	tie plate
6	11	downcomer	0.219911		18	
7	11		0.294961	hot leg nozzle	18	
8	30	inlet nozzle	0.294961		18	
9			0.246091		18	
10			0.270526		29	lower core
11			0.270526		29	support plate
12			0.257436		25	
13			0.257436		5	diffuser plate
14			0.244346		30	
15			0.270526	hot inlet nozzle	30	
16			0.270526		10	lower core plate
17			0.244346		20	active core inlet
18			0.219911		300	
19			0.294961	hot leg nozzle	300	
20			0.294961		150	
21			0.246091		105	
22			0.270526		70	nozzles
23			0.270526		25	
24			0.257436		250	

Table 4. The Boundary Conditions for Each Case

Run ID	Test ID	T <sup>c</sup> (K)	T <sup>c</sup> (°C)	T <sup>h</sup> (K)	T <sup>h</sup> (°C)	V <sup>c</sup> (l/m)	V <sup>h</sup> (l/m)	v <sup>c</sup> (m/s)	v <sup>h</sup> (m/s)	Pressure (atm)
1	2	324.6	51.45	334.6	61.45	180	180	0.78	0.78	3
2	5	381.4	108.25	391.7	118.55	250	250	1.08	1.08	3
3	8	332.2	59.05	342.3	69.15	310	310	1.34	1.34	3
4	11	349.1	75.95	359.2	86.05	350	350	1.52	1.52	3
5	14	339.1	65.95	349.6	76.45	310	310	1.34	1.34	5
6	17	335.3	62.15	345.6	72.45	310	310	1.34	1.34	7
7	20	376.9	103.75	390.0	116.85	180	310	0.78	1.34	3



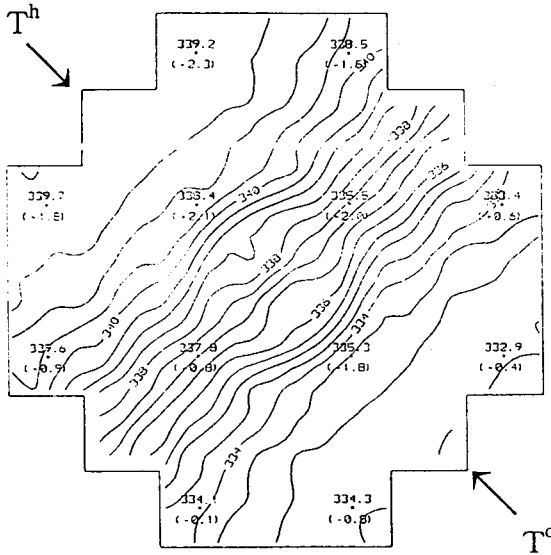


Fig. 11. COMMIX-1B Simulation of Test 8  
(3atm., 310l/min,  $T^h=342.3K$ ,  $T^c=332.2K$ )

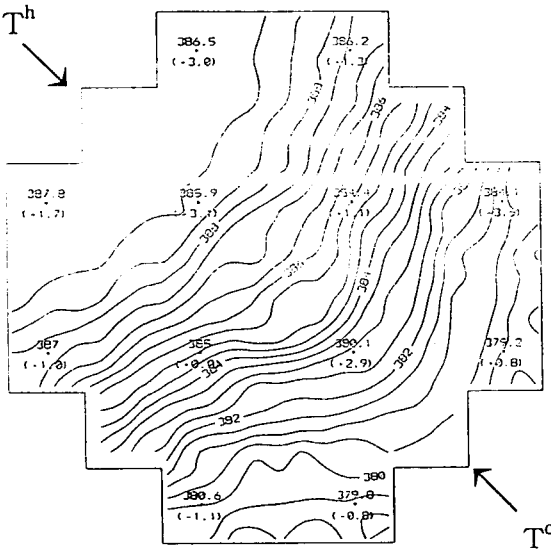


Fig. 12. COMMIX-1B Simulation of Test 20  
(3atm., 310l/min, 180l/min,  $T^h=390.0K$ ,  $T^c=376.9K$ )

ed on 96 points. Consequently the test results produce the isothermal lines highly dependent on the data points. Thus the isothermal lines based on the calculation results are more credible.

Nevertheless, the simulation results are very similar to test results as shown in Table 5. Thus the ability of COMMIX-1B code to simulate the coolant mixing phenomena in the lower plenum is verified.

### 5. Conclusion

The complete coolant mixing never occurs in the reactor vessel at any condition and mixing pattern is strongly dependent on the geometry of the lower plenum rather than the operating conditions or the accident circumstances.

The steady-state three-dimensional analysis of these tests using the COMMIX-1B computer code is performed and it is found that detailed modeling of the various structures in the lower plenum yields generally good agreement with the test data. Most of the thermal mixing trends at the entrance to the core are correctly computed by COMMIX-1B. Thus it is concluded that the COMMIX-1B code has sufficient capability to predict the coolant mixing pattern in nuclear plants having complex geometry of lower plenum.

So far the core inlet temperature model used in accident analysis is very simple; cold leg temperature for the region adjacent to cold leg and average temperature for the center region. Hence it is expected that when analysing the accident using the more accurate model of core inlet temperature distribution the safety margins should be increased.

Table 5. Maximum Temperature Difference Between Test and Calculation

Run ID	1	2	3	4	5	6	7
Maximum Temperature Difference(°C)	+2.8	+3.6	+2.3	+2.5	+2.7	+2.4	+3.1
	-0.3	-1.7	-1.8	-1.1	-1.8	-1.7	-1.1

## References

1. J.H. Kim, *Thermal Mixing in the Lower Plenum and Core of a PWR*, EPRI NP-3545. May (1984)
2. L.H. Kim, *Analysis of Oconee Unit 1 Downcomer and Lower Plenum Thermal-Mixing Tests Using COMMIX-1A*, EPRI NP-3780. November (1984)
3. K.H. Kim, *An Experimental Study on Natural Circulation in a UTSG PWR*, M.S. Thesis, SNU.
4. F.M. White, *Fluid Mechanics 2nd edition*, McGraw-Hill. (1986)
5. *Handbook of Product Manual*, Analog Device. (1991)
6. T.D. Radcliff, W.S. Johnson, J.R. Parsons, D.E. Ekeroth, "Visualization of the Lower Plenum Anomaly in the Westinghouse AP600 Reactor", *Heat Transfer and Fluid Flow*. (1993)
7. W.T. SHA, et. al., *COMMIX-1B: A Three-Dimensional Transient Single-phase Computer Program For Thermal Hydraulic Analysis Of Single And Multicomponent Systems*, NUREG/CR-4348, ANL-85-42. September (1985)

## Nomenclature

$A$	flow area at the throat of orifice
$D$	diameter of cold leg
$d$	diameter of orifice
$Q$	volumetric flow rate
$Re_D$	Reynolds number at cold leg
$T_{avg}$	average coolant temperature at core inlet
$T^c$	temperature for failed cold leg
$T^h$	temperature for intact cold leg
$V^c$	coolant flow rate for failed cold leg
$V^h$	coolant flow rate for intact cold leg
$v^c$	coolant velocity for failed cold leg
$v^h$	coolant velocity for intact cold leg
$\beta$	$d/D$
$\Delta p$	pressure difference across orifice
$\Delta T_c$	temperature difference between cold legs
$\rho$	density
$\sigma$	standard deviation of core inlet temperature